4086–4096 *Nucleic Acids Research, 2012, Vol. 40, No. 9* *Published online 11 January 2012*
doi:10.1093/nar/gkr1254

BC1-FMRP interaction is modulated by 2′-*O*-methylation: RNA-binding activity of the tudor domain and translational regulation at synapses

Caroline Lacoux[1,2,3,4], Daniele Di Marino[1,2,3], Pietro Pilo Boyl[2,3], Francesca Zalfa[1,5], Bing Yan[2,3], Maria Teresa Ciotti[6], Mattia Falconi[7], Henning Urlaub[8], Tilmann Achsel[2,3], Annie Mougin[4], Michèle Caizergues-Ferrer[4] and Claudia Bagni[1,2,3,*]

[1]Department of Experimental Medicine and Biochemical Sciences, Faculty of Medicine, University of Rome Tor Vergata, Via Montpellier, 1. 00133, Rome, Italy, [2]Catholic University of Leuven, Herestraat 49, ON&4. 3000 Leuven, Belgium, [3]VIB Center for the Biology of Disease, Katholieke Universiteit Leuven, ON&4. Herestraat, 49. 3000 Leuven, Belgium, [4]Universite' Paul Sabatier, Centre National de la Recherche Scientifique, Laboratoire de Biologie Moleculaire Eucaryote, 118, route de Narbonne. 31062, Toulouse, France, [5]University Campus Bio-Medico, Via Alvaro de Portillo, 21. 00128. Rome, Italy, [6]Consiglio Nazionale delle Ricerche/Centro Europeo per la Ricerca sul Cervello (CERC), Via del Fosso di Fiorano, 64. 00143 Rome, Italy, [7]Department of Biology, Faculty of Sciences, University of Rome Tor Vergata, Via della Ricerca Scientifica 1. 00133 Rome, Italy and [8]Max Planck Institute for Biophysical Chemistry, Am Fassberg 11. 37077 Goettingen, Germany

Received July 4, 2011; Revised November 8, 2011; Accepted December 2, 2011

ABSTRACT

The brain cytoplasmic RNA, *BC1*, is a small non-coding RNA that is found in different RNP particles, some of which are involved in translational control. One component of *BC1*-containing RNP complexes is the fragile X mental retardation protein (FMRP) that is implicated in translational repression. Peptide mapping and computational simulations show that the tudor domain of FMRP makes specific contacts to *BC1* RNA. Endogenous *BC1* RNA is 2′-*O*-methylated in nucleotides that contact the FMRP interface, and methylation can affect this interaction. In the cell body *BC1* 2′-*O*-methylations are present in both the nucleus and the cytoplasm, but they are virtually absent at synapses where the FMRP–*BC1*–mRNA complex exerts its function. These results strongly suggest that subcellular region-specific modifications of *BC1* affect the binding to FMRP and the interaction with its mRNA targets. We finally show that *BC1* RNA has an important role in translation of certain mRNAs associated to FMRP. All together these findings provide further insights into the translational regulation by the FMRP–*BC1* complex at synapses.

INTRODUCTION

Absence of the fragile X mental retardation protein (FMRP) causes the fragile X syndrome. FMRP is a multi-functional RNA-binding protein with roles in localization, translation (1,2) and stability of mRNAs (3,4). At synapses, two FMRP complexes have been identified: FMRP forms mRNPs with non-coding RNAs such as the brain cytoplasmic RNAs *BC1*/*BC200* (5,6) and the miRNAs (7). FMRP interacts with *BC1* RNA through its N-terminal region shown to contain a novel RNA-binding domain (8,9) containing two tudor motifs (10). The tudor domain has been described to typically recognize methylated amino acids (11). One activity of FMRP is to repress local translation (1,2), a process implicated in synapse maturation, learning and memory (12).

BC1 RNA is a small non-protein coding RNA (sncRNA) initially identified in rat brain (13,14) that is highly expressed in neurons (15,16) and enriched at synapses (17). *BC1* RNA forms diverse ribonucleoprotein particles (RNPs) with different protein partners including

*To whom correspondence should be addressed. Tel: +39 0672596063, +32 16330944; Fax: +3216330939; Email: claudia.bagni@uniroma2.it; claudia.bagni@cme.vib-kuleuven.be
Present address:
Pietro Pilo Boyl, Institut of Genetics, University of Bonn, Karlrobert-Kreiten-Str 13. 53115. Bonn, Germany.

FMRP (5,9,18), the Testis–Brain Protein (TBP) (19), Staufen (20), Pur alpha and beta (21), poly(A)-binding protein 1 (PABP1) (22,23), eIF4A (24) and hnRNPA2 (25). Some of the *BC1* RNP particles are involved in neuronal translational control as well; in particular, the FMRP–*BC1* complex represses translation of a defined subset of FMRP target mRNAs (5,6). In this context, *BC1* RNA acts as a bridging molecule between FMRP and the substrate mRNAs (5,18) and helps recruiting additional factors that are responsible for translation inhibition (6).

We show here that *BC1* RNA is 2′-*O*-methylated in the 5′-hairpin that is involved in mRNA translational regulation *in vivo* (5). These 2′-*O*-methylations are not detected at synapses where absence of *BC1* RNA affects translation of some FMRP target mRNAs. Peptide mapping, molecular modelling and docking simulations showed that the second tudor domain of FMRP recognizes the modified region of *BC1* RNA and surprisingly the 2′-*O*-methylations affect the interaction of *BC1* RNA with FMRP.

We propose that the 2′-*O*-methyl modifications of *BC1* RNA influence its activity in controlling translation at synapses.

MATERIALS AND METHODS

Details of general molecular procedures, RNA quantification by RT–qPCR and the primer sequences used in this study may be found in the Supplementary Data.

Animal care

Animal care was conducted conforming to the institutional guidelines that are in compliance with national and European laws and policies. Mouse strains that have been used in this study are: C57BL/6-129SV Wild-Type (WT) and C57BL/6-129SV *BC1* Knock-Out (KO). All animals used in this study were 3 weeks old.

Detection of 2′-*O*-methylations

2′-*O*-methylation was analysed as previously reported (26–28). Fifteen microgram of total RNA from WT mouse brain or 2 μg of synaptosomal RNA (highly enriched for *BC1* RNA, Supplementary Figure S1B) were used for each primer extension assay with low (4 and 2 μM) or high (1 mM) deoxyribonucleotide triphosphate (dNTP) concentration. 2′-*O*-methylation creates a primer extension stop when the dNTPs are limiting (4 and 2 μM, Supplementary Figure S2A). Avian Myeloblastosis Virus (AMV) reverse transcriptase (Q-biogen) and radiolabelled primers were used in the primer extension assays. Reverse transcription for RT–qPCR reactions used the Moloney Murine Leukemia Virus reverse transcriptase from Invitrogen. For the sequence of the oligos used, see Supplementary Data.

RNA sequencing

Two hundred nanogram of *BC1* and *U2* transcripts were sequenced using AMV reverse transcriptase (Q-biogen). The RNAs were denatured for 10 min at 70°C and renatured for 10 min on ice. The RT reactions were performed at 45°C for 35 min in the presence of 0.5 mM of each ddATP, ddGTP, ddCTP and ddTTP, and stopped with blue/formamide buffer. The RNA was denatured for 1 min at 90°C before being loaded onto an 8 M urea–10% polyacrylamide gel. The gel was then dried and exposed for 12 or 24 h using a PhosphoImager screen (GE Healthcare).

Expression of the FMRP-NT

Two separate sources of FMRP-N Terminus (FMRP-NT) were used. Independent experiments were performed using the FMRP protein domains prepared according to Zalfa *et al.* (9), produced in house, and the same protein domains produced by the Protein Expression and Purification Core Facility of the EMBL, Heidelberg.

Mutagenesis of the FMRP-N Terminus

In order to mutagenize the FMRP-NT, we used the Quick Change Lightning Multi Site-Directed Kit (from Quiagen) and the pET-M11-FMRP-NT plasmid which has the same insert as described in (9), cloned into NcoI-KpnI site of pET-M11 (EMBL protein expression group).

To generate the R70E-R11E double mutant, the DNA oligos TV1 and TV2 were used. Mutagenized triplet is shown in bold.

TV1: 5′ - GGTTTATTCC**GAA**GCAAATGAAAAAG-3′

TV2: 5′ - GTCACAATTGAG**GAG**CTACGATCTG - 3′

To generate the Y103A-N104A double mutant, the DNA oligo TV5 was used. Mutagenized triplets are shown in bold.

TV5: 5′- GTGATGCTACG**GCTGCT**GAAATTGTC ACAATTG 3′

The two mutagenized plasmids were sequenced before use.

Electrophoretic mobility shift assay

BC1 RNA was *in vitro* transcribed in the presence of α-[^{32}P] UTP using T7 RNA polymerase, or reconstituted by ligation of [^{32}P]-labelled oligos in the presence of a splint DNA oligo (29) (Supplementary Data). Directly before use, RNAs were denatured/renatured in electrophoretic mobility shift assay (EMSA) buffer in the presence of 1 μg of tRNAs. Then, 1×10^5–2×10^5 cpm of RNA (corresponding to 10 and 20 fmol, respectively) were incubated with 1–5 pmoles of FMRP N-terminus for 20 min at room temperature in the presence of 150 mM KCl, 5 mM $MgCl_2$, 2 mM DTT, 5% glycerol, 20 mM HEPES, pH 7.6 and 1 μg yeast tRNA. The entire reaction (20 μl) was loaded on a native 1 × TBE/6% acrylamide gel and run in 0.5× TBE from 2 to 4 h at 170 V in a cold room. The autoradiogram was recorded with a PhosphorImager (GE Healthcare) and the bands were quantified. From the equation $K_d = ([R][P]/[RP]) \rightarrow [RP]/[R] = [P]/K_d$, the ratio of [bound RNA]/[free RNA] was plotted against [P], the slope giving $1/K_d$.

Sucrose gradients to separate mRNPs and polysomes

Total mouse brain was homogenized in 3 ml of lysis buffer (10 mM Tris–HCl pH 7.5, 100 mM NaCl, 10 mM $MgCl_2$,

1% Triton X-100, 1 mM dithiothreitol DTT, 30 U/ml RNasin). After 5 min of incubation on ice, the extract was centrifuged for 4 min at 9300 g at 4°C. The supernatant (up to 0.5 ml) was frozen in liquid N_2 and either stored at −80°C or immediately loaded onto a 15–50% (w/v) sucrose gradient and centrifuged at 4°C for 1 h 50 min at 37 000 rpm in a Beckman SW41 rotor. Same procedure was used to isolate Polysomes and mRNPs from synaptoneurosomes. See Supplementary Data for Polysome-mRNP analysis.

Synaptoneurosome preparation and RNA extraction

Synaptoneurosomes are particles containing both pre- and postsynaptic compartments (30). Synaptoneurosomes were prepared as previously described (6). Details can be found in Supplementary Data.

Nuclear and cytoplasmic extracts

Cortices were weighed and resuspended in fractionation buffer (75 mg in 600 µl). Nuclear and cytoplasmic extracts were prepared using the PARIS kit according to manufacturer's recommendation (Ambion). RNA quality control was performed using the Experion system (Bio-Rad).

Immunoprecipitation followed by RT–PCR and RT–qPCR analysis

Total brain and synaptosomes were lysed in 100 mM NaCl, 10 mM $MgCl_2$, 10 mM Tris–HCl pH 7.5, 1% Triton X-100, 1 mM DTT, 40 U/ml RNAse OUT (Invitrogen), 10 µl/µl Protease inhibitor cocktail (Sigma-Aldrich), 5 mM β-glycerophosphate, 0.5 mM Na_3VO_4. After 5 min of incubation on ice, lysates were centrifuged for 5 min at 12 000 *g* at 4°C. The protein concentration was determined and the equivalent of 500 µg protein of the supernatant was used for the IP using anti-FMRP antibodies (16) or purified rabbit IgGs as negative control, and protein A Dynabeads (Invitrogen). RT–PCR and RT–qPCR were performed as described in Supplementary Data.

Mass spectrometric analysis of UV cross-links

The FMRP–*BC1* particles (5 nmol of FMRP-NT and 10 nmol of *BC1* RNA) were incubated in EMSA-binding buffer for 15 min on ice and irradiated on glass dishes at 254 nm with four 8-Watt germicidal lamps (G8T5, Herolab, Wiesloch, Germany) in parallel at a distance of 4 cm for 2 min on ice.

The reactions were diluted with buffer containing 1 M of urea, and digested with trypsin, RNase A and RNase T1. Peptides cross-linked to an RNA moiety were enriched on TiO_2, and analysed by Electro Spray Ionization Quadrupole Time Of Flight as described by (31–33). Cross-linked peptides exhibit the combined mass of the peptide and the RNA fragment; in the Q-TOF sequencing, the cross-linked amino acid is identified as the one where the sequencing ladder breaks off.

Computational procedures

The MC-Sym web server (http://www.major.iric.ca/MC-Sym/) has been used to generate the atomic structure of the *BC1* 5′-end RNA (34). As a template we used the *BC1* 5′-hairpin 2D structure experimentally determined by Rozhdestvensky and collaborators (35). This analysis, i.e. the secondary structure determined by chemical and enzymatic assays, revealed that *BC1* RNA 5′-domain has an extended rod-like stem-loop structure. Details regarding the molecular modelling and the molecular docking procedures can be found in Supplementary Data.

RESULTS AND DISCUSSION

BC1 RNA represses translation of FMRP mRNA targets at synapses

BC1 RNA is highly localized in dendrites and axons and it is thought to regulate local protein synthesis (5,36). Previous reports have shown a functional interaction between *BC1* RNA and FMRP at synapses (5,9,37,38). To investigate the contribution of *BC1* RNA to FMRP-mediated translational regulation, we performed polysome-mRNP gradient analysis. Cytoplasmic whole-brain extracts from 3 weeks old WT and *BC1* KO mice (39) were fractionated on continuous sucrose gradients. Figure 1A shows the sedimentation profiles for the two genotypes. Fractions that contain actively translating polysomes (P) and translationally silent mRNPs (mRNPs), respectively, were pooled and the extracted RNAs were used to determine the translational efficiency by RT–qPCR (as percentage of mRNAs on polysomes, PMP, Figure 1B) of *Arc*, *αCamKII* and *Map1B* mRNAs that are translationally controlled by FMRP (5,40–44). When the polysomal-mRNP analysis was carried out from total brain, no increase in the PMP value was observed for *Arc*, *αCamKII* and *Map1B* mRNAs (Figure 1C). These data show that in total brain of *BC1* KO animals, the translational efficiency of some FMRP target mRNAs is not altered compared to WT (Figure 1C).

We then investigated whether loss of *BC1* RNA affects mRNA translation at synapses. Synaptoneurosomes (30) from WT and *BC1* KO mice were prepared as previously described (6). The quality of the preparations was verified by the enrichment of synaptic proteins and RNAs (Supplementary Figure S1A and S1B). The PMP of *Arc*, *αCamKII* and *Map1B* mRNAs resulted higher in synaptoneurosomes from *BC1* KO animals than in their WT littermates (Figure 1D), showing that these mRNAs are more efficiently translated in the absence of *BC1* RNA at synapses similarly to what we observed in synaptoneurosomes from *Fmr1* KO mice (5). Western blot analysis confirmed the increased level of proteins encoded by those mRNAs at synapses (Figure 1F), meanwhile no protein increase is observed in total brain (Figure 1E). These data suggest that *BC1* RNA controls the translation of three FMRP mRNA targets mainly at synapses and this nicely coincides with the observation of

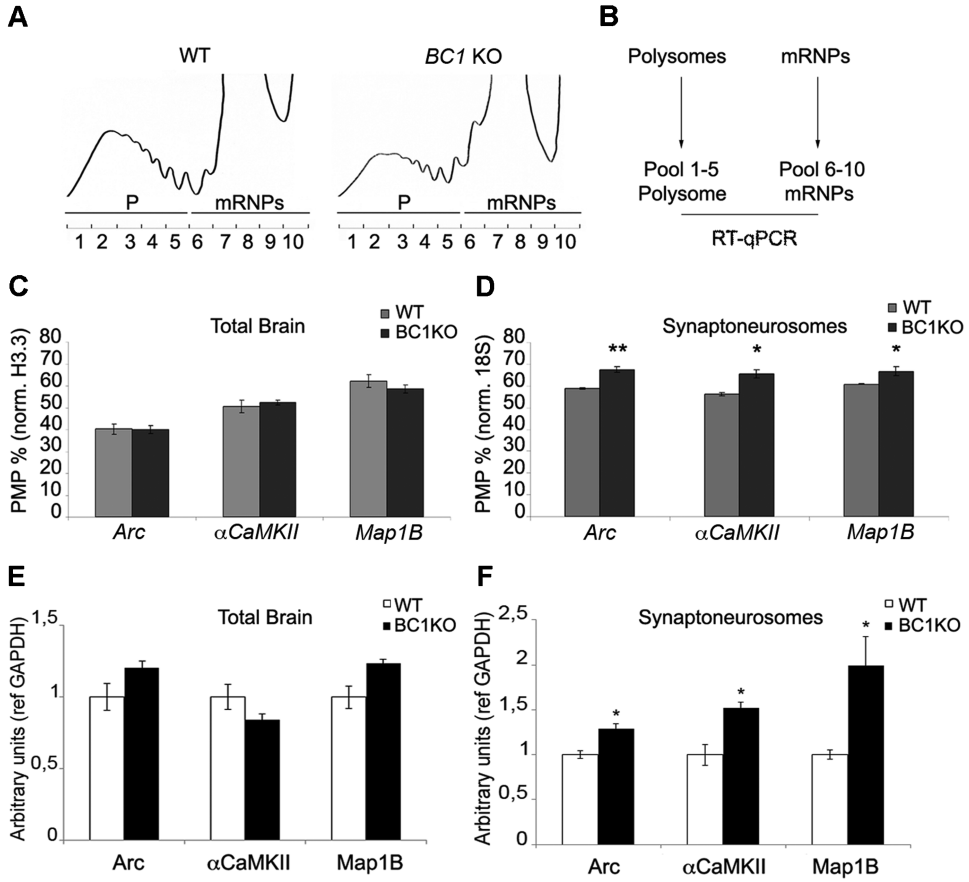

Figure 1. *BC1* RNA represses mRNA translation at synapses. (**A**) Cytoplasmic brain extracts from WT and *BC1* KO mice were centrifuged through a 15–50% sucrose gradient; absorbance at 254 nm was monitored continuously and plotted against the fraction numbers. (**B**) Fractions 1–5, corresponding to polysomes (P) and the fractions 6–10 containing mRNPs (mRNP) were pooled and further analysed by RT–qPCR. (**C**) Translational efficiency of *Arc*, *αCaMKII* and *Map1B* mRNAs from WT (grey histograms) and *BC1* KO (black histograms) mice were quantified and expressed as PMP in the histograms. (**D**) Same as in panel (C) using synaptosomal preparation. Error bars represent SE: $*P < 0.05$ or $**P < 0.01$ for *BC1* KO versus WT by Student's test, $n = 4$. (**E**) Protein levels of Arc, αCaMKII and Map1B from WT (in white) and *BC1* KO (in black) from total brain. (**F**) Same as in (E) using synaptic protein extracts. Error bars represent SE: $*P < 0.05$ for KO versus WT by Student's test, $n = 3$.

a translation dysregulation in synaptoneurosomes from *Fmr1* KO mice (5). These findings strongly suggest that the FMRP/*BC1* RNP exerts its major function at synapses.

BC1 RNA is differentially 2′-*O*-methylated in neurons

Post-transcriptional RNA modifications can have important roles in modulating its functions by influencing secondary and tertiary structure (45,46). Endogenous *BC1* RNA was therefore isolated from mouse brain and examined for the presence of 2′-*O*-methylation, one of the most common RNA modifications. The analysis was performed on the *BC1* 5′-hairpin that is implicated in the interaction with FMRP and its target mRNAs (5,9).

We first verified the efficacy of the previously established methodology (26–28) by analysing, in mouse brain, the well-documented *U2* snRNA 2′-*O*-methylations (47) (Supplementary Figure S2A). Using the *BC1*-specific primers BMN155 and BMN297 (Figure 2A) and total brain RNA, 2′-*O*-methylations were clearly detected in the 5′-stem-loop at positions G46 (Gm46), C47 (Cm47) and G56 (Gm56) (Figure 2B and C: compare lanes 5 and 6; 2′-*O*-methylations are detected by strong signals with less dNTPs, $n = 5$). No 2′-*O*-methylations were observed using *in vitro*-transcribed *BC1* RNA (Figure 2B and C, lanes 11 and 12 and lanes 7 and 8, respectively), or in the region located between the two hairpins of the endogenous *BC1* RNA (nucleotides 75–127, data not shown). Since the FMRP–*BC1* complex controls mRNA translation at synapses (5,6) (Figure 1D and F) we prepared synaptoneurosomes in order to analyse the 2′-*O*-methylation status of *BC1* RNA at synapses. In this case, no 2′-*O*-methylations were detected on the synaptic *BC1* RNA (Figure 2B and C, compare lanes 13, 14 and 9 and 10, respectively, $n = 4$). The presence of intact *BC1* RNA molecules was verified by the presence of a stop of elongation at nucleotide 1 of *BC1* RNA (Supplementary Figure S2B). Because *BC1* RNA was found differentially 2′-*O*-methylated in the cell body versus the synapses, we investigated its methylation status in the nucleus. Nuclear and cytoplasmic compartments, used for this analysis, were revealed by the presence and enrichment for dyskerin and Glyceraldehyde 3-phosphate

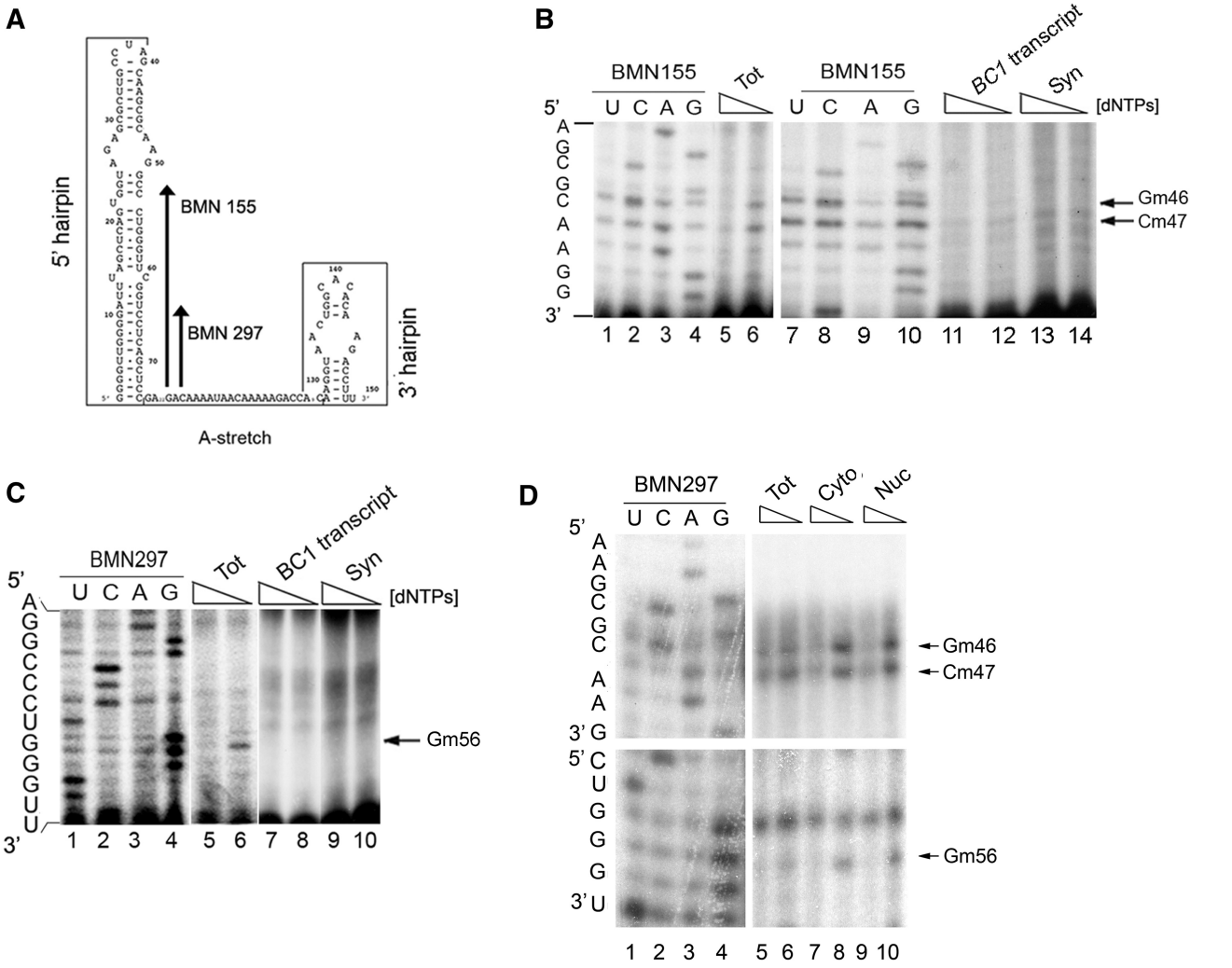

Figure 2. *BC1* RNA is 2′-*O*-methylated. (**A**) Primers used to detect *BC1* RNA 2′-*O*-methylations: BMN297, BMN155 are indicated on the *BC1* secondary structure. (**B**) Low dNTP concentration primer extension analysis using the BMN155 primer on total brain RNA from WT mice (lanes 5 and 6), on the *BC1* transcript (lanes 11 and 12), and on RNA from synaptoneurosomes (lanes 13 and 14). The arrows denote 2′-*O*-methylations at positions G46, C47. For each sample, the second lane shows the lower dNTP concentration; stops due to low dNTP indicate the presence of a 2′-*O*-methylation. Sequencing reactions are shown in lanes 1–4 and 7–10. (**C**) Same as in (**B**) using the BMN297 primer; sequencing (lanes 1–4), low dNTP concentration primer extension analysis on total brain (lanes 5 and 6), on *BC1* transcript (lanes 7 and 8) and on synaptosomal preparation (lanes 9 and 10). (**D**) Same as in (C) using total brain (lanes 5 and 6), cytoplasmic (lanes 7 and 8) and nuclear extracts (lanes 9 and 10).

dehydrogenase (Supplementary Figure S1C). As shown in Figure 2D, *BC1* RNA from the cytoplasmic or nuclear fractions is 2′-*O*-methylated (compare lanes 7 and 8 and lanes 9 and 10 for cytoplasmic and nuclear fraction, respectively) underlining that absence of these 2′-*O*-methylations may have a function at synapses. These findings suggest that *BC1* 2′-*O*-methylations occur in nucleus.

To our knowledge this is the first time that a non-coding RNA is shown to be differently modified according to its subcellular location.

BC1 RNA 2′-*O*-methylations affect FMRP binding

Since the unmodified *BC1* RNA is present at synapses, where the FMRP–*BC1* complex acts as a translational inhibitor, we studied this interaction further.

The N-terminus of FMRP (FMRP-NT; residues 1–217) contains two tudor domains (10), has RNA-binding properties (8,48), and interacts directly with the *BC1* 5′-hairpin (5,9). Because FMRP-NT tends to aggregate (48) (and data not shown) we tested its correct folding via the binding to the entire unmodified *BC1* RNA (Figure 3A and B) as well as to poly riboG and poly riboC (data not shown). The FMRP-NT binds *BC1* RNA with high affinity (apparent $K_d = 128 \pm 22.7$ nM, the same within experimental error as in ref. (9); see Figure 3A for the gel and Supplementary Figure S3A for the K_d plot). Furthermore, a similarly structured RNA, *U1* snRNA, was unable to compete with *BC1* RNA for the FMRP binding (Figure 3B, compare lane 2 with lanes 4, 5 and 6).

In order to gain insights into the FMRP-NT/*BC1* interaction, we cross-linked *BC1* RNA to FMRP-NT by UV exposure, enriched the tryptic peptides that were covalently bound to RNA, and analysed them by mass

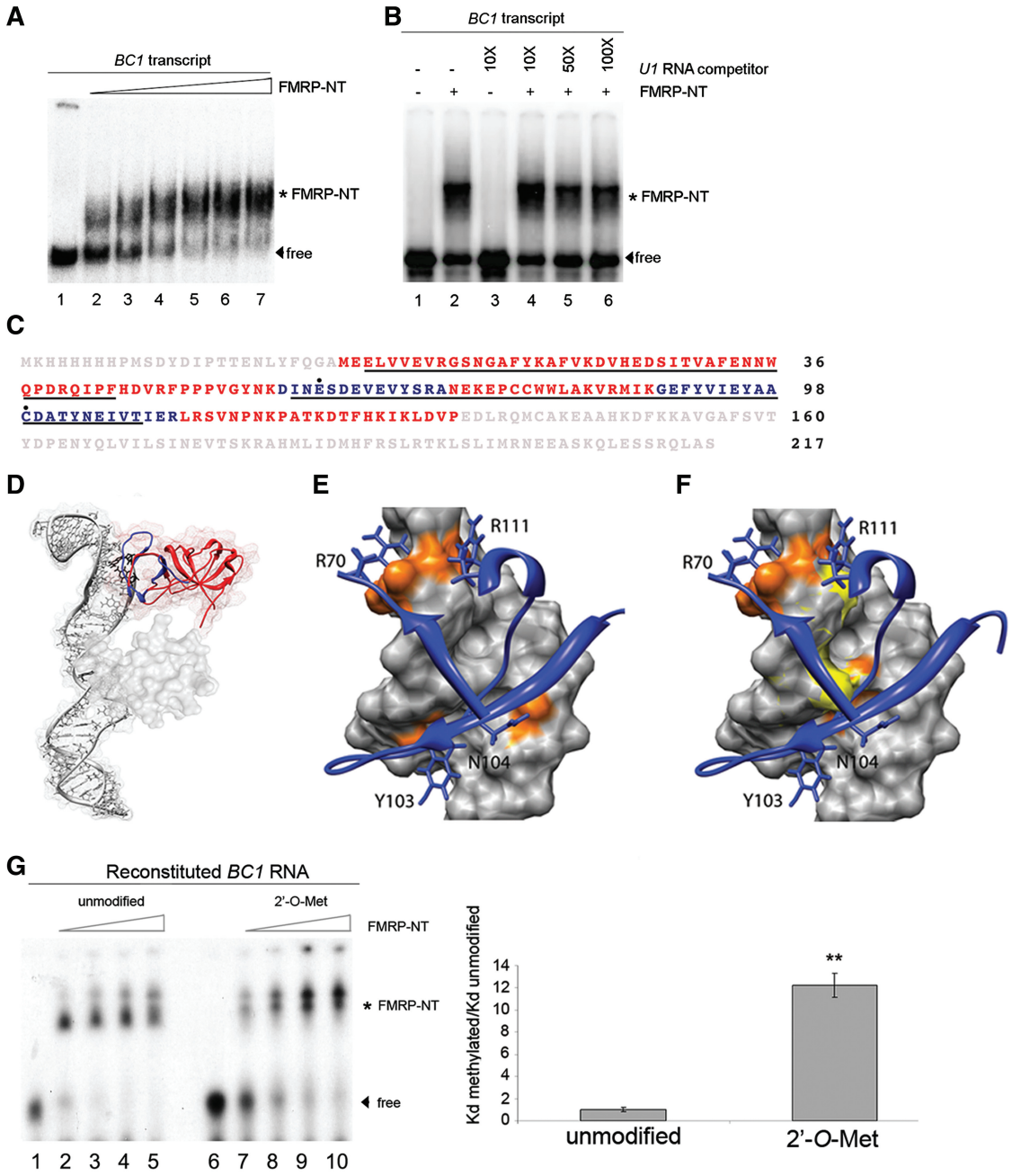

Figure 3. Functional mapping of the FMRP-NT/*BC1* interaction. (**A**) EMSA using the entire *BC1* RNA without (lane 1) or with increasing amounts of FMRP-NT (from 20 to 500 ng, lanes 2–7). The asterisk denotes the shifted FMRP–*BC1* complex. Arrowhead denotes unbound *BC1* (free). (**B**) Competition experiment using unlabelled *U1* RNA. Lane 1 radiolabelled *BC1* RNA, lane 2 radiolabelled *BC1* and FMRP-NT (100 ng, asterisk). Lanes 4 and 6 show binding of FMRP-NT and *BC1* RNA in the presence of 10–100-fold excess of unlabelled *U1* RNA. Lanes 1 and 3 do not contain FMRP-NT. (**C**) Identification of FMRP residues that are in contact with *BC1* RNA. The two tudor domains are underlined in black. The tryptic peptides containing the cross-linked amino acids (highly reactive: E61 and C99, black dots) are shown in blue. (**D**) Docking model of the interaction of FMRP-NT with the 5′-end of *BC1*. The backbone of the tudor domains is shown in red, with the two cross-linked peptides highlighted in blue. (**E** and **F**) Electrostatic and hydrogen-bond interactions of the FMRP-NT with *BC1* RNA. FMRP is shown as a blue ribbon, and the lateral chains of the amino acids involved in the binding network are indicated as blue sticks. The RNA is shown as grey molecular surface with the nucleotides involved in the hydrogen bond and electrostatic network (orange spot), the 2′-*O*-methylated atoms are shown as a yellow surface. (**G**) EMSA using FMRP-NT (from 25 to 100 ng) and unmodified *BC1* RNA (lanes 2–5) or 2′-*O*-methylated *BC1* RNA (lanes 7–10). Lanes 1 and 6, unbound *BC1* RNA. The asterisk indicates the FMRP-NT/*BC1* RNA complex. The histogram shows the ratio of the K_d of 2′-*O*-methylated *BC1* construct versus the K_d of unmodified *BC1* construct. Error bars represent SE: $^{**}P < 0.01$, Student's test, $n = 3$.

spectrometry using a recently described methodology (31–33) in which mass spectroscopy sequencing identifies the cross-linked amino acid. The two amino acids that cross-link to *BC1* RNA are indicated in Figure 3C (E61 and C99, black dots) and are both situated in the second tudor domain (underlined). Next we carried out a molecular modelling of the *BC1* RNA tertiary structure. Based on this structure, the 3D structure of the first 134 amino acids of FMRP-NT (10), and the cross-links identified by mass spectrometry (Figure 3C, blue peptides), we performed a molecular docking simulation to generate a protein–RNA complex (Figure 3D). The molecular docking simulation shows that the hypothesized recognition between FMRP-NT and 5′-end *BC1* RNA is stabilized through both salt bridges and hydrogen-bond interactions. Specifically the FMRP residues R70, Y103, N104 and R111 interact through hydrogen bonds with the RNA nucleotides G31, C32, C45, G46, C47 and A48 (Figure 3E, orange nucleotides and Supplementary Table S1). Furthermore, salt bridge interactions occur between the two arginines R70 and R111 and the phosphate groups of the nucleotides C47 and A48 (Figure 3E and Supplementary Table S1). Importantly, two of the three 2′-*O*-methylated nucleotides (G46 and C47) are directly involved in FMRP-NT binding while the third (G56) is localized outside of this binding region. When two methyl groups are added, by molecular modelling, to the nucleotides G46 and C47 (Figure 3F, methyl groups in yellow), significant changes in the *BC1* surface occur that affect the interaction with FMRP-NT. In particular, the addition of 2′-*O*-methylations increases the steric hindrance and makes access of FMRP more difficult (Figure 3F). In order to characterize the effect of *BC1* 2′-*O*-methylations on FMRP binding, the *BC1* 5′-hairpin was synthesized in an unmodified or 2′-*O*-methylated form, ligated to the *BC1* 3′-end (A-stretch plus 3′-hairpin) to constitute the entire *BC1* RNA (Supplementary Figure S3B) and tested for its ability to associate to FMRP-NT. As shown in Figure 3G, the 2′-*O*-methylated *BC1* RNA binds significantly less to FMRP-NT (right panel: the K_d of the 2′-*O*-methylated *BC1* RNA oligonucleotide is ~10-fold higher than the K_d of the unmodified one). 2′-*O*-methylation of these nucleotides in the minimal FMRP-binding domain of *BC1* confirmed these data (Supplementary Figure S3C). We suggest that the 2′-*O*-methylation critically alters the *BC1* surface shape and, reducing the electrostatic interactions, decreases the affinity between FMRP-NT and *BC1*.

While the tudor domains of FMRP are necessary for RNA binding, they are not sufficient: another 83 amino acids are needed to create the RNA-binding domain (9). We could not model this extra domain with high confidence, because there are no reference structures showing sufficient identity in the databases. However, molecular docking suggests that this domain might be able to form additional contacts to the basis of the 5′-hairpin. In particular, the helix-loop-helix (HLH) motif in this region (10) might insert itself into the major groove of the RNA region containing the third 2′-*O*-methylated nucleotide (G56), creating additional specific contacts (Figure 3D and data not shown). It is thus the second tudor domain of FMRP together with the adjacent residues that creates a novel RNA-binding surface. A crucial contribution to the binding comes from R70 and R111 that form salt bridges to the negative charges of the phosphates at positions 47 and 48. While these contacts are formed by the tudor domain, its canonical methyl binding site is not involved in the RNA binding. Instead, the tudor domain serves as a scaffold that positions the amino acids on one site of the beta barrel in such away that they can form specific interactions with the *BC1* RNA.

Structural analysis of the FMRP-NT/*BC1* interaction

According to the molecular docking simulation and the experimental cross-linking data, the second tudor domain gives an important contribution to the stability of the FMRP-NT/*BC1* complex. In order to verify this model, two different FMRP-NT double mutants were created. In the first mutant the positive charge, carried by the side chain of residues R70 and R111 (Figure 3E and F), was reversed by mutating both the residues into glutamic acid, while in the second mutant the hydrogen-bond interactions of residues Y103 and N104 (Figure 3E and F) were removed by mutating both residues into alanines. The effect of these mutations was predicted by docking simulation, comparing the HADDOCK score (49) where a lower value predicts stronger binding.

The introduction of two alanines at positions 103 and 104 actually removes the hydrogen bonds formed by the wild type residues (compare Figure 4A and C and see Supplementary Table S1). Due to the reduced steric hindrance of the alanine residues, however, the FMRP protein wraps more tightly around *BC1* RNA improving other energy terms in the HADDOCK score (i.e. the van der Waals, the buried surface area, the binding and the desolvation energies). The total score therefore decreases from −38.0 in the WT to −49.0 in the mutant, predicting a higher binding affinity. The docking model was experimentally validated by EMSA experiments with the *in vitro*-transcribed unmodified *BC1* RNA and the mutant protein (produced in *Escherichia coli*; Supplementary Figure S4A). As expected, the apparent K_d decreases by a factor of 2.7 (Figure 4F, strong tendency: $P = 0.07$, $n = 5$; apparent K_d FMRP NT WT = 128 ± 22.7 nM and K_d NT Mut = 51 ± 4.1 nM) showing the validity of the modelling. On the other hand the reversion of the positive charges (R70E-R111E, Figure 4A and B) repel the negatively charged phosphates of the RNA backbone, leading to a change in the FMRP orientation towards *BC1* and thus to a considerable decrease in the area of interaction surface (Figure 4B). Therefore, the HADDOCK score increases from −38.0 to −25.0, showing a significantly lower affinity. Again the docking prediction was verified by EMSA using the mutant protein (Supplementary Figure S4B). The K_d increased significantly by a factor of 3.8 (Figure 4D, $P < 0.01$, $n = 3$. Apparent K_d FMRP NT WT = 128 ± 22.7 nM and K_d FMRP NT Mut = 488 ± 12 nM, respectively). Competition experiments, using both unlabelled *BC1* and *U1* RNAs, showed that the mutated

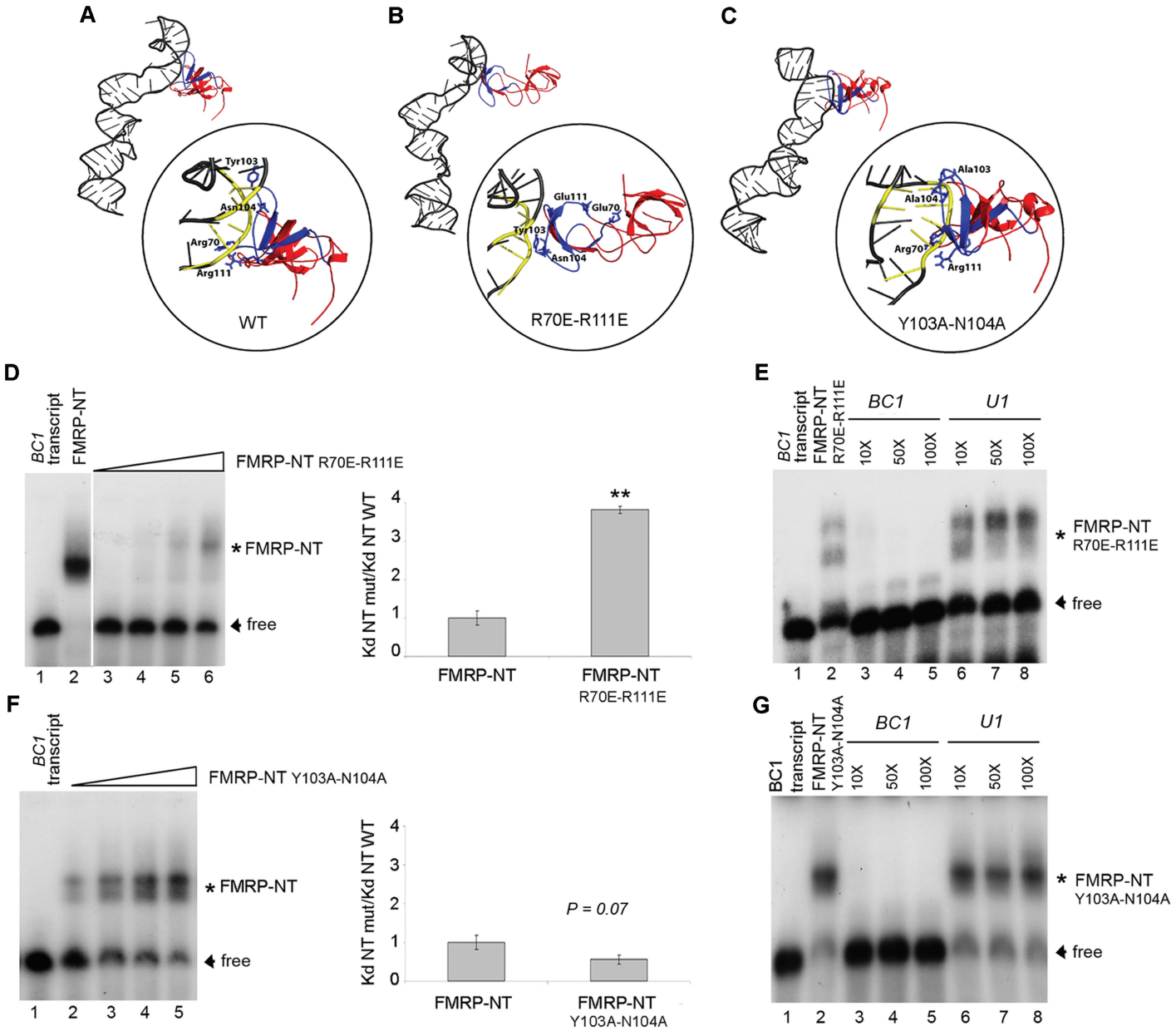

Figure 4. Effect of R70, R111, N104, Y103 to the binding of *BC1* RNA. (**A–C**) Docking models of the FMRP-NT WT, FMRP-NT R70E-R111E and FMRP-NT Y103A-N104A interaction with *BC1*, respectively. The yellow RNA backbone represents the nucleotides involved in the interaction. The key amino acids detected by mass spectrometry analysis are depicted as blue sticks. (**D**) EMSA experiment using *BC1* RNA, FMRP-NT WT and FMRP-NT R70E-R111E mutant (10–100 ng). Shifted and unbound RNA are indicated by asterisk and arrowhead, respectively; the histogram shows the ratio of the K_d of mutant FMRP-NT versus the K_d of WT FMRP-NT. Error bars represent SE: $^{**}P < 0.01$, Student's test, $n = 3$. (**E**) Competition experiments using unlabelled *BC1* (lanes 3–5) and *U1* (lanes 6–8) transcripts. (**F**) and (**G**) The same as in (D) and (E) but using the Y103A-N104A mutant. $P = 0.07$ Student's test, $n = 5$.

FMRP-NT/*BC1* interaction remains specific (Figure 4E and G). In conclusion the electrostatic interactions of the two arginines R70 and R111 guide the interaction of the second tudor domain with *BC1* RNA. Interestingly the binding partners of the two arginines are the phosphates at the 3′-side of the 2′-*O*-methylated nucleotides G46 and C47.

The FMRP–*BC1*–mRNA inhibitory complex at synapses

To investigate if *BC1* 2′-*O*-methylations have an effect on the affinity of FMRP for its mRNA targets, we immunoprecipitated FMRP complexed with *BC1* RNA from total brain (Figure 5A, left panel). At first, we monitored that *BC1* RNA was indeed associated to FMRP (Figure 5A, right panel), together with a well-known FMRP target (*αCaMKII* mRNA). The specificity of the interaction is revealed by the absence of *D2DR* mRNA in the FMRP complex (38). To address whether the *BC1* bound to FMRP is 2′-*O*-methylated or not, we performed low dNTP primer extension assays from FMRP immunoprecipitated RNAs (Figure 5B). Using the *BC1*-specific primers, BMN155 and BMN297, the

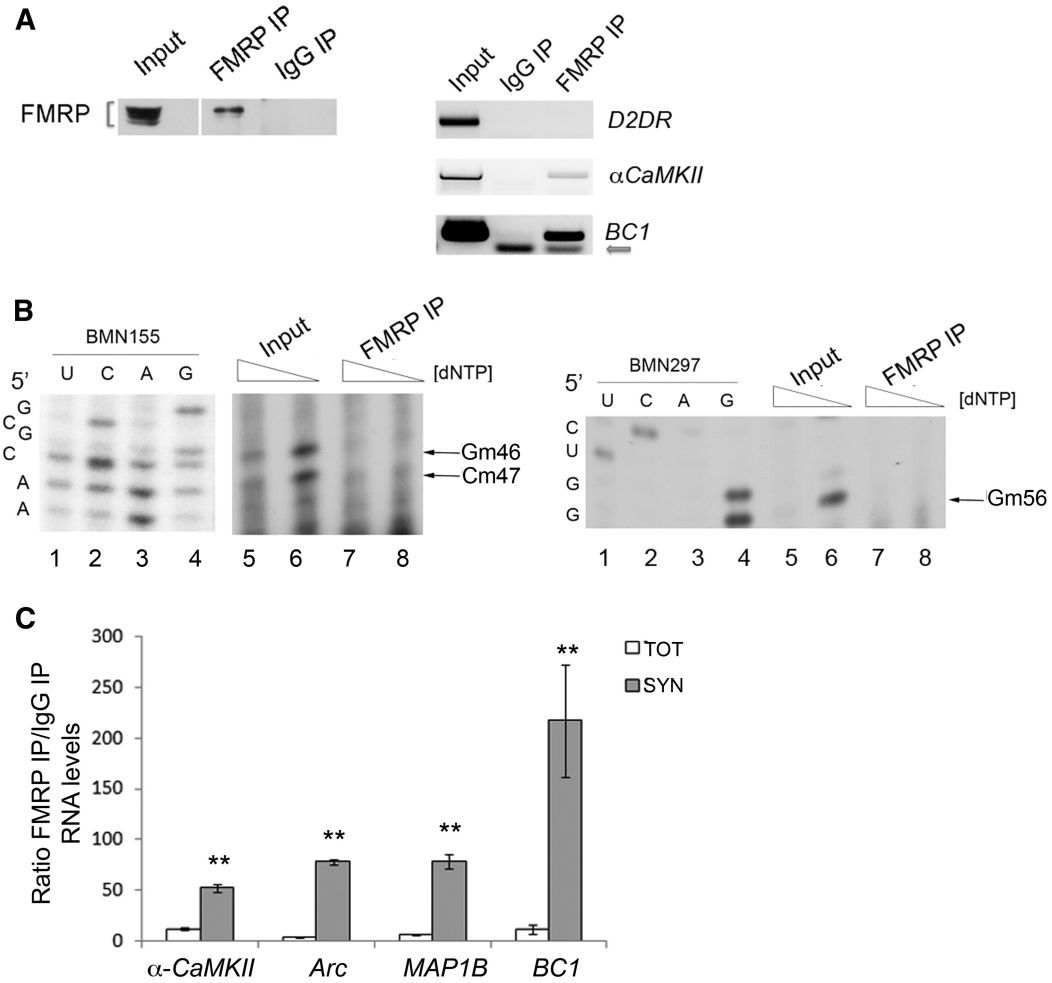

Figure 5. At synapses, where *BC1* is mainly unmethylated, FMRP binds its mRNA targets with higher affinity. (**A**) Immunoprecipitation of FMRP-associated mRNAs/RNA. Left panel, Western blot of FMRP immunoprecipitated from total brain extracts. Input (1/10), FMRP IP (1/3), the IgG IP (1/3). Right panel, RT–PCR from immunoprecipitated RNA derived from the input (1/10), IgG IP (2/3) and FMRP IP (2/3). The arrow points to the primers used to amplify *BC1* RNA (**B**) Upper panel, low dNTP concentration primer extension analysis using the BMN155 primer on total brain RNA (Input, lanes 5 and 6) and immunoprecipitated *BC1* RNA (lanes 7 and 8, $n = 5$). The arrows denote 2′-*O*-methylations at positions G46, C47. For each sample, the second lane shows the lower dNTP concentration. Sequencing reactions are shown in lanes 1–4. Lower panel as upper panel using the BMN297 primer able to detect the 2′-*O*-methylation on the G56, $n = 3$. (**C**) Enrichment of FMRP mRNA targets in immunoprecipitated FMRP complex from both total brain and at synapses. RT–qPCR of FMRP co-immunoprecipitated mRNAs/RNA. Shown is the ratio of the RNA precipitated using FMRP and rabbit unspecific IgGs from total (white histogram) and synaptoneurosomes (grey histogram) brain extracts, each normalized for the respective input. Error bars represent SE: $^{**}P < 0.01$, Student's test, $n = 3$.

2′-*O*-methylations were detected in the 5′-stem-loop only in the input RNA (Figure 5B, left and right panels: compare lanes 5 and 6) while the *BC1* immunoprecipitated by FMRP was not 2′-*O*-methylated (Figure 5B: compare lanes 7 and 8). Since the *in vitro* data showed that FMRP binds less efficiently to 2′-*O*-methylated *BC1* RNA (Figure 3G, Supplementary Figure S3C), we wanted to investigate if the presence or absence of 2′-*O*-methylations on *BC1* RNA had also an effect on stabilizing FMRP target mRNAs in the complex. To address this point we immunoprecipitated FMRP from total brain and synaptoneurosomal extracts and detected the associated mRNAs in the complex. RT–qPCR assays showed a higher co-immunoprecipitation efficiency of FMRP target mRNAs/RNA *(αCamKII, Arc, Map1B, BC1*) in synaptoneurosome preparations versus total brain (Figure 5C, Supplementary Figure S5). Since at synapses *BC1* is mainly detected in the non-methylated form, these findings suggest that absence of 2′-*O*-methylations favours the FMRP–*BC1*–mRNA association. Importantly, this complex has been previously shown *in vivo* to inhibit mRNA translation at synapses (5,6) and Figure 1D and F).

In conclusion, in this study, we show that (i) *BC1* is differentially 2′-*O*-methylated according to its subcellular location. (ii) The tudor domain of FMRP, with its RNA-binding activity, binds FMRP recognizing the 2′-*O*-methylation status of *BC1* RNA. (iii) At synapses, where *BC1* RNA is not 2′-*O*-methylated, the FMRP–*BC1*–mRNA interaction is increased. (iv) At synapses *BC1* regulates the translation of some FMRP target mRNAs.

At structural level, methylation of the sugar 2′-OH-group favour the 3′-endo conformation which stabilize helical conformations (46). It is possible to envision that the endo-conformation affects the binding to a given protein. In a highly complex cell like the neuron, which undergoes many changes during brain development, elaborate and fine-tuned mechanisms are required to regulate gene expression. We propose that changes in the 2′-*O*-methylation status of *BC1* RNA contribute to the regulation of synaptic gene regulation and consequently neuronal plasticity.

These findings provide new insights into translational control at synapses and suggest that RNA modifications could have an important influence in genetic brain disease, a heretofore unknown relationship.

SUPPLEMENTARY DATA

Supplementary Data are available at NAR Online: Supplementary Table 1, Supplementary Figures 1–5, Supplementary Methods and Supplementary References [3,6,16,29,49,50–54].

ACKNOWLEDGEMENTS

The authors thank Tamas Kiss (CNRS, LBME, Toulouse, France) for plasmids expressing *U1* and *U2* snRNAs, Eliane Cherrette for assistance, Jonathan Royaert for technical help, Emanuela Pasciuto for sharing preliminary data and Hüseyin Besir, Giuseppe Novelli and Maria-Giulia Farace for access to facilities, Silvia De Rubeis and Esperanza Fernandez for comments on the article.

FUNDING

Telethon (GGP10150); Fonds Wetenschappelijk Onderzoek (G066709N); Vlaams Instituut Voor Biotechnologie and European Union Seventh Framework Programme under grant agreement n° (HEALTH-F4-2010-242167 "SynSys" project) (to C.B.); Methusalem (to B.D.S.); the National Autism Association Research (NAAR) (to C.L.) and European Molecular Biology Organization (ASTF 170-2008 to C.L.). Funding for open access charge: Telethon.

Conflict of interest statement. None declared.

REFERENCES

1. Bagni,C. and Greenough,W.T. (2005) From mRNP trafficking to spine dysmorphogenesis: the roots of fragile X syndrome. *Nat. Rev. Neurosci.*, **6**, 376–387.
2. Bassell,G.J. and Warren,S.T. (2008) Fragile X syndrome: loss of local mRNA regulation alters synaptic development and function. *Neuron*, **60**, 201–214.
3. Zalfa,F., Eleuteri,B., Dickson,K.S., Mercaldo,V., De Rubeis,S., di Penta,A., Tabolacci,E., Chiurazzi,P., Neri,G., Grant,S.G. *et al.* (2007) A new function for the fragile X mental retardation protein in regulation of PSD-95 mRNA stability. *Nat. Neurosci.*, **10**, 578–587.
4. Zhang,M., Wang,Q. and Huang,Y. (2007) Fragile X mental retardation protein FMRP and the RNA export factor NXF2 associate with and destabilize Nxf1 mRNA in neuronal cells. *Proc. Natl Acad. Sci. USA*, **104**, 10057–10062.
5. Zalfa,F., Giorgi,M., Primerano,B., Moro,A., Di Penta,A., Reis,S., Oostra,B. and Bagni,C. (2003) The fragile X syndrome protein FMRP associates with BC1 RNA and regulates the translation of specific mRNAs at synapses. *Cell*, **112**, 317–327.
6. Napoli,I., Mercaldo,V., Boyl,P.P., Eleuteri,B., Zalfa,F., De Rubeis,S., Di Marino,D., Mohr,E., Massimi,M., Falconi,M. *et al.* (2008) The fragile X syndrome protein represses activity-dependent translation through CYFIP1, a new 4E-BP. *Cell*, **134**, 1042–1054.
7. Edbauer,D., Neilson,J.R., Foster,K.A., Wang,C.F., Seeburg,D.P., Batterton,M.N., Tada,T., Dolan,B.M., Sharp,P.A. and Sheng,M. (2010) Regulation of synaptic structure and function by FMRP-associated microRNAs miR-125b and miR-132. *Neuron*, **65**, 373–384.
8. Adinolfi,S., Ramos,A., Martin,S.R., Dal Piaz,F., Pucci,P., Bardoni,B., Mandel,J.L. and Pastore,A. (2003) The N-terminus of the fragile X mental retardation protein contains a novel domain involved in dimerization and RNA binding. *Biochemistry*, **42**, 10437–10444.
9. Zalfa,F., Adinolfi,S., Napoli,I., Kuhn-Holsken,E., Urlaub,H., Achsel,T., Pastore,A. and Bagni,C. (2005) Fragile X mental retardation protein (FMRP) binds specifically to the brain cytoplasmic RNAs BC1/BC200 via a novel RNA-binding motif. *J. Biol. Chem.*, **280**, 33403–33410.
10. Ramos,A., Hollingworth,D., Adinolfi,S., Castets,M., Kelly,G., Frenkiel,T.A., Bardoni,B. and Pastore,A. (2006) The structure of the N-terminal domain of the fragile X mental retardation protein: a platform for protein-protein interaction. *Structure*, **14**, 21–31.
11. Maurer-Stroh,S., Dickens,N.J., Hughes-Davies,L., Kouzarides,T., Eisenhaber,F. and Ponting,C.P. (2003) The Tudor domain 'Royal Family': Tudor, plant Agenet, Chromo, PWWP and MBT domains. *Trends Biochem. Sci.*, **28**, 69–74.
12. Costa-Mattioli,M., Sossin,W.S., Klann,E. and Sonenberg,N. (2009) Translational control of long-lasting synaptic plasticity and memory. *Neuron*, **61**, 10–26.
13. Sutcliffe,J.G., Milner,R.J., Bloom,F.E. and Lerner,R.A. (1982) Common 82-nucleotide sequence unique to brain RNA. *Proc. Natl Acad. Sci. USA*, **79**, 4942–4946.
14. Milner,R.J., Bloom,F.E., Lai,C., Lerner,R.A. and Sutcliffe,J.G. (1984) Brain-specific genes have identifier sequences in their introns. *Proc. Natl Acad. Sci. USA*, **81**, 713–717.
15. Muslimov,I.A., Lin,Y., Heller,M., Brosius,J., Zakeri,Z. and Tiedge,H. (2002) A small RNA in testis and brain: implications for male germ cell development. *J. Cell Sci.*, **115**, 1243–1250.
16. Ferrari,F., Mercaldo,V., Piccoli,G., Sala,C., Cannata,S., Achsel,T. and Bagni,C. (2007) The fragile X mental retardation protein-RNP granules show an mGluR-dependent localization in the post-synaptic spines. *Mol. Cell. Neurosci.*, **34**, 343–354.
17. Chicurel,M.E., Terrian,D.M. and Potter,H. (1993) mRNA at the synapse: analysis of a synaptosomal preparation enriched in hippocampal dendritic spines. *J. Neurosci.*, **13**, 4054–4063.
18. Johnson,E.M., Kinoshita,Y., Weinreb,D.B., Wortman,M.J., Simon,R., Khalili,K., Winckler,B. and Gordon,J. (2006) Role of Pur alpha in targeting mRNA to sites of translation in hippocampal neuronal dendrites. *J. Neurosci. Res.*, **83**, 929–943.
19. Muramatsu,T., Ohmae,A. and Anzai,K. (1998) BC1 RNA protein particles in mouse brain contain two y-,h-element-binding proteins, translin and a 37 kDa protein. *Biochem. Biophys. Res. Commun.*, **247**, 7–11.
20. Mallardo,M., Deitinghoff,A., Muller,J., Goetze,B., Macchi,P., Peters,C. and Kiebler,M.A. (2003) Isolation and characterization of Staufen-containing ribonucleoprotein particles from rat brain. *Proc. Natl Acad. Sci. USA*, **100**, 2100–2105.
21. Kobayashi,S., Agui,K., Kamo,S., Li,Y. and Anzai,K. (2000) Neural BC1 RNA associates with pur alpha, a single-stranded DNA and RNA binding protein, which is involved in the transcription of the BC1 RNA gene. *Biochem. Biophys. Res. Commun.*, **277**, 341–347.

22. Muddashetty,R., Khanam,T., Kondrashov,A., Bundman,M., Iacoangeli,A., Kremerskothen,J., Duning,K., Barnekow,A., Huttenhofer,A., Tiedge,H. *et al.* (2002) Poly(A)-binding protein is associated with neuronal BC1 and BC200 ribonucleoprotein particles. *J. Mol. Biol.*, **321**, 433–445.
23. Kondrashov,A.V., Kiefmann,M., Ebnet,K., Khanam,T., Muddashetty,R.S. and Brosius,J. (2005) Inhibitory effect of naked neural BC1 RNA or BC200 RNA on eukaryotic in vitro translation systems is reversed by poly(A)-binding protein (PABP). *J. Mol. Biol.*, **353**, 88–103.
24. Wang,H., Iacoangeli,A., Popp,S., Muslimov,I.A., Imataka,H., Sonenberg,N., Lomakin,I.B. and Tiedge,H. (2002) Dendritic BC1 RNA: functional role in regulation of translation initiation. *J. Neurosci.*, **22**, 10232–10241.
25. Muslimov,I.A., Iacoangeli,A., Brosius,J. and Tiedge,H. (2006) Spatial codes in dendritic BC1 RNA. *J. Cell Biol.*, **175**, 427–439.
26. Maden,B.E. (2001) Mapping 2′-O-methyl groups in ribosomal RNA. *Methods*, **25**, 374–382.
27. Motorin,Y., Muller,S., Behm-Ansmant,I. and Branlant,C. (2007) Identification of modified residues in RNAs by reverse transcription-based methods. *Methods Enzymol.*, **425**, 21–53.
28. Yu,Y.T., Shu,M.D. and Steitz,J.A. (1997) A new method for detecting sites of 2′-O-methylation in RNA molecules. *RNA*, **3**, 324–331.
29. Stark,M.R., Pleiss,J.A., Deras,M., Scaringe,S.A. and Rader,S.D. (2006) An RNA ligase-mediated method for the efficient creation of large, synthetic RNAs. *RNA*, **12**, 2014–2019.
30. De Rubeis,S. and Bagni,C. (2009) In: Binder,M.D., Hirokawa,N., Windhorst,U. and Hirsch,M.C. (eds), *Encyclopedia of Neuroscience*. Springer, Part 19. pp. 3982–3985.
31. Kuhn-Holsken,E., Lenz,C., Dickmanns,A., Hsiao,H.H., Richter,F.M., Kastner,B., Ficner,R. and Urlaub,H. (2010) Mapping the binding site of snurportin 1 on native U1 snRNP by cross-linking and mass spectrometry. *Nucleic Acids Res.*, **38**, 5581–5593.
32. Lenz,C., Kuhn-Holsken,E. and Urlaub,H. (2007) Detection of protein-RNA crosslinks by NanoLC-ESI-MS/MS using precursor ion scanning and multiple reaction monitoring (MRM) experiments. *J. Am. Soc. Mass Spectrom.*, **18**, 869–881.
33. Martin Richter,F., Hsiao,H.H., Plessmann,U. and Urlaub,H. (2009) Enrichment of protein-RNA crosslinks from crude UV-irradiated mixtures for MS analysis by on-line chromatography using titanium dioxide columns. *Biopolymers*, **91**, 297–309.
34. Parisien,M. and Major,F. (2008) The MC-Fold and MC-Sym pipeline infers RNA structure from sequence data. *Nature*, **452**, 51–55.
35. Rozhdestvensky,T.S., Kopylov,A.M., Brosius,J. and Huttenhofer,A. (2001) Neuronal BC1 RNA structure: evolutionary conversion of a tRNA(Ala) domain into an extended stem-loop structure. *RNA*, **7**, 722–730.
36. Cao,X., Yeo,G., Muotri,A.R., Kuwabara,T. and Gage,F.H. (2006) Noncoding RNAs in the mammalian central nervous system. *Annu. Rev. Neurosci.*, **29**, 77–103.
37. Gabus,C., Mazroui,R., Tremblay,S., Khandjian,E.W. and Darlix,J.L. (2004) The fragile X mental retardation protein has nucleic acid chaperone properties. *Nucleic Acids Res.*, **32**, 2129–2137.
38. Centonze,D., Rossi,S., Napoli,I., Mercaldo,V., Lacoux,C., Ferrari,F., Ciotti,M.T., De Chiara,V., Prosperetti,C., Maccarrone,M. *et al.* (2007) The brain cytoplasmic RNA BC1 regulates dopamine D2 receptor-mediated transmission in the striatum. *J. Neurosci.*, **27**, 8885–8892.
39. Skryabin,B.V., Sukonina,V., Jordan,U., Lewejohann,L., Sachser,N., Muslimov,I., Tiedge,H. and Brosius,J. (2003) Neuronal untranslated BC1 RNA: targeted gene elimination in mice. *Mol. Cell. Biol.*, **23**, 6435–6441.
40. Brown,V., Jin,P., Ceman,S., Darnell,J.C., O'Donnell,W.T., Tenenbaum,S.A., Jin,X., Feng,Y., Wilkinson,K.D., Keene,J.D. *et al.* (2001) Microarray identification of FMRP-associated brain mRNAs and altered mRNA translational profiles in fragile X syndrome. *Cell*, **107**, 477–487.
41. Zhang,Y.Q., Bailey,A.M., Matthies,H.J., Renden,R.B., Smith,M.A., Speese,S.D., Rubin,G.M. and Broadie,K. (2001) Drosophila fragile X-related gene regulates the MAP1B homolog Futsch to control synaptic structure and function. *Cell*, **107**, 591–603.
42. Lu,R., Wang,H., Liang,Z., Ku,L., O'Donnell,W.T., Li,W., Warren,S.T. and Feng,Y. (2004) The fragile X protein controls microtubule-associated protein 1B translation and microtubule stability in brain neuron development. *Proc. Natl Acad. Sci. USA*, **101**, 15201–15206.
43. Park,S., Park,J.M., Kim,S., Kim,J.A., Shepherd,J.D., Smith-Hicks,C.L., Chowdhury,S., Kaufmann,W., Kuhl,D., Ryazanov,A.G. *et al.* (2008) Elongation factor 2 and fragile X mental retardation protein control the dynamic translation of Arc/Arg3.1 essential for mGluR-LTD. *Neuron*, **59**, 70–83.
44. Hou,L., Antion,M.D., Hu,D., Spencer,C.M., Paylor,R. and Klann,E. (2006) Dynamic translational and proteasomal regulation of fragile X mental retardation protein controls mGluR-dependent long-term depression. *Neuron*, **51**, 441–454.
45. Helm,M. (2006) Post-transcriptional nucleotide modification and alternative folding of RNA. *Nucleic Acids Res.*, **34**, 721–733.
46. Motorin,Y. and Helm,M. (2010) tRNA stabilization by modified nucleotides. *Biochemistry*, **49**, 4934–4944.
47. Massenet,S., Mougin,A. and Branlant,C. (1998) In: Grosjean,H. and Benne,R. (eds), *Post-Transcriptional Modifications in the U Small Nuclear RNAs*. ASM Press, Washington DC, pp. 201–227.
48. Adinolfi,S., Bagni,C., Musco,G., Gibson,T., Mazzarella,L. and Pastore,A. (1999) Dissecting FMR1, the protein responsible for fragile X syndrome, in its structural and functional domains. *RNA*, **5**, 1248–1258.
49. Dominguez,C., Boelens,R. and Bonvin,A.M. (2003) HADDOCK: a protein-protein docking approach based on biochemical or biophysical information. *J. Am. Chem. Soc.*, **125**, 1731–1737.
50. Hoe,H.S., Fu,Z., Makarova,A., Lee,J.Y., Lu,C., Feng,L., Pajoohesh-Ganji,A., Matsuoka,Y., Hyman,B.T., Ehlers,M.D. *et al.* (2009) The effects of amyloid precursor protein on postsynaptic composition and activity. *J. Biol. Chem.*, **284**, 8495–8506.
51. Sheng,M. (2001) Molecular organization of the postsynaptic specialization. *Proc. Natl Acad. Sci. USA*, **98**, 7058–7061.
52. Hoareau-Aveilla,C., Bonoli,M., Caizergues-Ferrer,M. and Henry,Y. (2006) hNaf1 is required for accumulation of human box H/ACA snoRNPs, scaRNPs, and telomerase. *RNA*, **12**, 832–840.
53. Vriend,G. (1990) WHAT IF: a molecular modeling and drug design program. *J. Mol. Graph.*, **8**, 52–56, 29.
54. Humphrey,W., Dalke,A. and Schulten,K. (1996) VMD: visual molecular dynamics. *J. Mol. Graph.*, **14**, 33–38, 27–38.